VNU Journal of Science: Natural Sciences and Technology

Journal homepage: https://js.vnu.edu.vn/NST

Original Article

Effects of Zn (II) on the Optical Properties of CdTe Quantum Dots and Their Photoluminescence Response to Lead Ion

Nguyen Thi Nhan, Vu Anh Duc, Mai Xuan Dung, Hoang Quang Bac[*]

Hanoi Pedagogical University 2,
32 Nguyen Van Linh, Xuan Hoa, Phuc Yen, Vinh Phuc, Vietnam

Abstract: Water-soluble CdTe quantum dots (QDs) have been utilized as photoluminescence probes for the detection of metal ions such as Pb^{2+}, Hg^{2+}, Cd^{2+}, etc. We initially developed highly photoluminescence (PL) Zn-doped CdTe for toxic ions detection. A study on the changes of optical properties of Zn-doped CdTe and CdTe QDs when exposed to Pb^{2+} suggested that Pb^{2+} could act as a surface passivating agent to reduce Te^{2-} dangling bonds while Zn^{2+} dopant stabilizes the QDs surface against ambient oxidation. The results demonstrated herein provide useful understandings of the interactions between water-soluble QDs and metal ions. These results suggest further applications of QDs in sensing metal ions.

Keywords: CdTe quantum dots, sensing, photoluminescence, metal ions, doping.

1. Introduction

CdTe quantum dots (QDs) are typical water-soluble QDs that have been deployed as photoluminescence (PL) probes for diverse applications including metal sensing [1-4], cell imaging [5, 6], and pesticide detection [7, 8]. In those applications, the PL intensity of QDs under constant excitation conditions usually decreases simultaneously with the concentration of the analyte. In the case of metal ion sensing, PL quenching by the ions has been widely reported and rationally attributed to

photo-induced electron transferring from QDs to the ions [3, 9, 10] or surface capping ligand detachment [4]. To be applicable as a PL probe, QDs must have stable PL quantum yield and suitable conduction band energy level (CBE). To the first issue, CdTe QDs are usually passivated with an inorganic shell to increase the stability toward environmental oxidation and a durable capping layer which is normally composed of thiolate or bidentate ligands. The inorganic shell could be a thin CdS layer that is grown by post-illumination deposition or thermal decomposition [11-14] or be CdS/ZnS multiple layers [15, 16]. To the second issue, CBE can be varied either by tuning the QDs size thanking to the quantum confinement effect or employing a capping ligand having different

hybridization with the frontier orbital of QDs [17, 18].

Based on the above considerations, we initially developed water-soluble, highly photoluminescence, and small-sized CdTe QDs for toxic metal ions detection. Zn^{2+} ions incorporated into CdTe QDs by using a mixture of Cd^{2+} and Zn^{2+} as metal resources were found to enhance the PL of QDs. Pb^{2+} was selected as a model ion for the study because according to the national technical regulation on drinking water quality (QCVN 01:2009/BYT), the permissible concentration of Pb is the third lowest value i.e., just below Hg and Cd among mentioned metals. Unexpectedly, Pb^{2+} with a concentration varying in nM to μM scale did not alter significantly the PL intensity of CdTe QDs but enhanced the emission intensity of Zn-doped CdTe QDs. We proposed that Pb^{2+} ions can act as Z-type ligands so that they can increase the emission efficiency by passivating surficial anions

2. Experimental Section

2.1. Chemicals

Chemicals including $CdCl_2.5/2H_2O$ (99.95%), Na_2TeO_3 (99.9%), glutathione (GSH, 98%), $ZnCl_2$ (99.99%), and $NaBH_4$ (98%) were purchased from Aladdin Chemicals and used without further purifications. Freshly prepared double-distillated water was used for the synthesis and dispersion of QDs while acetone was used to precipitate QDs during the purification process.

2.2. The Synthesis and Purification of Quantum Dots

Telluride solution was first prepared in N_2-filled flask by mixing 0.04 g of Na_2TeO_3¬ with 0.07 g of NaBH4 dissolved in 5 ml of water. In a separated flask, 0.35 g of GSH was added into 50 ml of $CdCl_2$ 0.02 M solution to form a thiolate complex. After degassing the thiolate solution via a Schlenk line system, the telluride solution was then injected and the pH of the combined solution was adjusted to 10.5

by adding NaOH 0.5 M solution. To prepare Zn-doped CdTe QDs (hereafter denoted as Zn-CdTe QDs), a mixture including 5 ml of $ZnCl_2$ 0.02 M and 45 ml of $CdCl_2$ 0.02 M solution was used. After pH adjustment, the combined solution was heated rapidly and refluxed for 10 minutes under N_2-filled condition followed by swiftly quenched by an ice bath. To purify QDs, acetone was added to precipitate QDs which were then collected by means of centrifugation before being dissolved in water. The precipitation - redispersion cycle was repeated three times followed by air drying to obtain dried QDs, which were stored in a refrigerator for further usages

2.3. Characterizations

UV-Vis absorption spectra of aqueous solutions of QDs as well as mixture solutions of QDs and Pb^{2+} were recorded on a UV-2450 (Shimadzu) spectrometer. PL spectra were carried out using a Nanolog (Horiba) spectrometer while transmission electron microscope (TEM) images of QDs were obtained on a JEM 2100 microscope.

3. Results and Discussion

TEM image of CdTe QDs is shown in Fig. 1a. QDs exhibited spherical shapes with a diameter ranging from 3 to 4.8 nm with an average diameter of about 3.5 nm. UV-Vis absorption spectra of CdTe and Zn-CdTe QDs are shown in Figure 1 b. For comparison, those two samples were selected so that they have a similar excitonic peak by adjusting the refluxing time, e.g. 7 minutes for CdTe QDs and 10 minutes for Zn-CdTe QDs, respectively. The first excitonic peak of CdTe QDs positioned at 478 nm while that of Zn-CdTe QDs maximized at 473 nm. The absorption spectra were normalized to the first excitonic peak.

Obviously, the absorption coefficient at the low-wavelength region, e.g. ~400 nm, which was reported to be size-independent [19], decreased when Zn^{2+} was incorporated into CdTe QDs Figure 1.

The decreased absorption coefficient caused by Zn^{2+} incorporation could be explained as follows. 4 s, 4 p, and 3 d electronic states of Zn in the valence band of ZnTe have lower energies than 5s, 5p, and 4d electronic states of Cd in CdTe [20]. Additionally, electronic states of Te including 5 s, 5 p, and 5 s are lower in ZnTe than those states in CdTe [20], probably due to the higher dissociation energy of the Zn-Te bond compared to the Cd-Te bond [21]. The changes in electronic states reduce the density of state near the conduction band edge of CdTe QDs, therefore reducing the absorption cross-section as mentioned above.
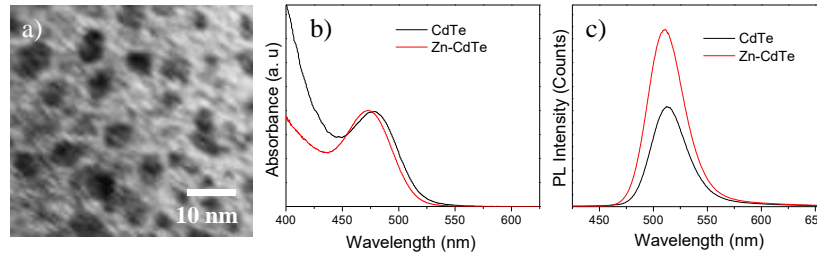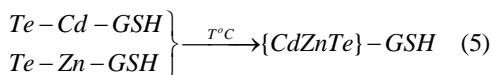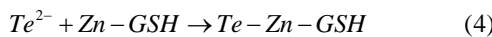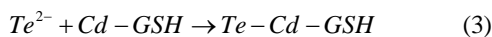

Figure 1. a) TEM image of CdTe quantum dots; b) UV-Vis absorption and c) PL spectra (excited at 400 nm) of CdTe and Zn-CdTe quantum dots.

PL spectra of CdTe and Zn-CdTe QDs are shown in Fig. 1c. Both types of QDs had a bell-shaped emission spectrum, maximized at ca. 512 nm, and did not exhibit surface-related emission at long-wavelength regions. It means that CdTe and Zn-CdTe QDs had good surface passivation. For comparison, spectra shown in Fig. 1c were obtained on two aqueous solutions having the same optical density at 400 nm of about 0.06. The emission yield of Zn-CdTe QDs was about 1.3 times greater than that of CdTe QDs. The effects of Zn^{2+} incorporation on PL enhancement of CdTe QDs have been widely reported and can be rationally summarized as follows:

$$Cd^{2+} + GSH \rightarrow Cd - GSH \qquad (1)$$

$$Zn^{2+} + GSH \rightarrow Zn - GSH \qquad (2)$$

$$Te^{2-} + Cd - GSH \rightarrow Te - Cd - GSH \qquad (3)$$

$$Te^{2-} + Zn - GSH \rightarrow Te - Zn - GSH \qquad (4)$$

$$\left. \begin{array}{l} Te - Cd - GSH \\ Te - Zn - GSH \end{array} \right\} \xrightarrow{T^{\circ}C} \{CdZnTe\} - GSH \quad (5)$$

Cd^{2+} and Zn^{2+} react with GSH resulting in thiolate complexes (eq. 1 and 2), which react with Te^{2-} forming molecular complexes where Te^{2-} ions act as a ligand (eq. 3 and eq. 4). Under refluxing conditions, those molecular complexes condense to form QD nuclei (eq. 5), which then grow to form QDs via Ostwald ripening process. Because Te^{2-} ion reacts faster with Cd-GSH than Zn-GSH [22] and the concentration of Cd^{2+} was much higher than Zn^{2+} the incorporation of Zn^{2+} into the QDs likely took place lately, resulting Zn-doped CdTe QDs with in Zn-rich surfaces. During the growth of QDs, the thiolate complexes could be decomposed, releasing S^{2-} ions that reasonably incorporate into CdTe growing crystals. The incorporation of S^{2-} ions made CdTe QDs be alike CdTe/CdS core/shell QDs while the deposition of Zn^{2+} and S^{2-} resulted in CdTe/ZnCdS core/multiple shell structures [6, 22-24]. Since the dissociation energy of Zn-X (X=Te, S) bonds are higher than Cd-X counterparts the presence of Zn^{2+} ion stabilized the surface of CdTe QDs giving rise to enhanced PL as aforementioned in Figure. 1 c.

To realize the application potential of CdTe QDs as PL probe for Pb^{2+} detection, we prepared mixture solutions of QDs with Pb^{2+} so that the optical density of the solutions was maintained and the concentration of Pb^{2+} varied around the permissible limit in drinking water, e.g. 0.01 ppm (or 4.8×10^{-8}M). PL spectra of those solutions are compared in Figure 2. As seen in Figure 2 a and 2 b, the presence of Pb^{2+}

reduced the emission intensity of CdTe QDs by about 15% and the PL reduction did not vary linearly with Pb^{2+} concentration. The PL intensity of Zn-CdTe QDs changed slightly with Pb^{2+} of about 5 nM and it enhanced by about 15% when the concentration of Pb^{2+}

increased to 10 or 100 nM. From the results shown in Figure. 2, we suggest that CdTe and Zn-CdTe QDs could be used as PL probes for the qualitative detection of Pb^{2+} in water by observing PL quenching or PL enhancement, respectively.
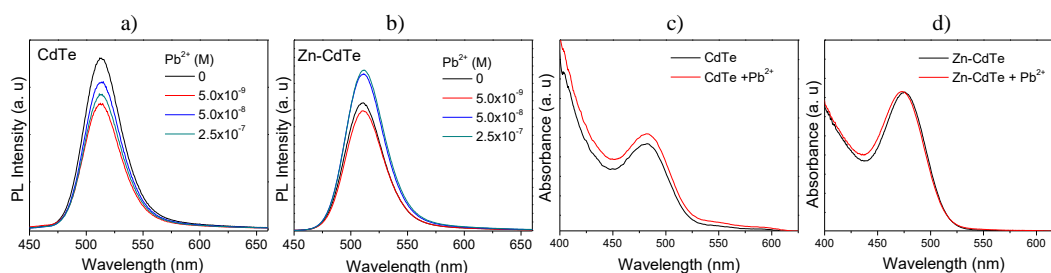

Figure 2. Effects of Pb^{2+} on the PL spectra (**a**): CdTe, **b**): Zn-CdTe) and the absorption spectra, (**c**):CdTe, **d**): Zn-CdTe) quantum dots. In **c**) and **d**) the concentration of Pb^{2+} was 1 mM and the spectra were recorded after 2 hours of reaction.
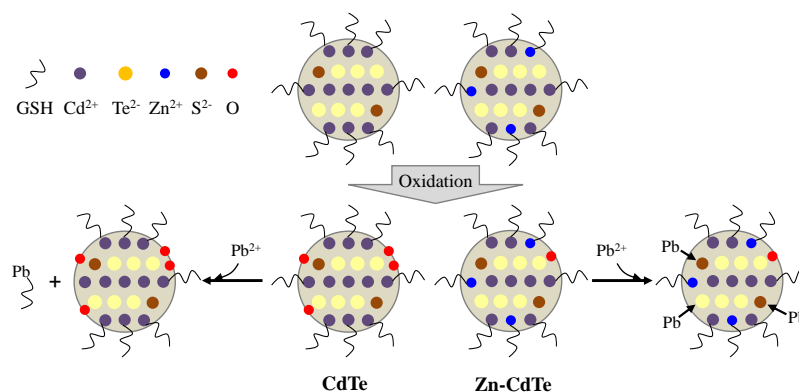

Figure 3. Proposal interaction mechanism between Pb^{2+} ions and quantum dots.

Because PbTe has a much lower bandgap than CdTe, the incorporation of Pb^{2+} into the CdTe QDs via the cationic exchanging process must red-shift the position of the first excitonic. As shown in Figure 2 c and 2 d, the first excitonic peaks of CdTe and Zn-CdTe were negligibly changed. Therefore, we discarded the PL changes observed in Figure 2 a and 2 b due to cation exchange. To explain the effects of Pb^{2+} ions on the PL of QDs we proposed a tentative mechanism as cartooned in Figure 3. During the storage state, QDs were partially oxidized [25]. The incorporation of Zn^{2+} and S^{2-} into the surfaces of QDs results in Zn-CdTe QDs that have a structure similar to

CdTe/ZnCdS core/multiple shells, which reduces the oxidation of Zn-CdTe as compared to CdTe QDs. Upon exposure to Pb^{2+} solution, unoxidized Te^{2-} or S^{2-} on the surfaces of Zn-CdTe QDs can be coordinated by Pb^{2+} ions (denoted at Pb→ in Figure 3). In this case, Pb^{2+} ions act as a Z-type ligand, additional passivating the QDs's surfaces to enhance the emission intensity as mentioned in Figure 2 b [26, 27]. Additionally, due to the higher affinity of Pb^{2+} to the thiol functional group than Cd^{2+} or Zn^{2+}, Pb^{2+} ions could also take some passivating GSH ligands of QDs leaving QDs's surfaces with unpassivated cations, which cause PL to decrease. These two opposite effects of

Pb^{2+} on the PL of QDs rationally explain why PL did not vary linearly with Pb^{2+} concentration as shown in Figure 2 a and 2 b. In the case of CdTe QDs, since Te^{2-} ions were partially oxidized, the PL enhancement induced by Pb^{2+} coordination was not very manifest as in the case of Zn-CdTe QDs. Consequently, the PL quenching effects of Pb^{2+} ions were dominant so that PL of CdTe QDs decreased as mentioned previously in Figure 2 a.

4. Conclusion

Green-emitting CdTe and Zn-CdTe QDs have been synthesized for Pb^{2+} ion detection. Optical characterizations revealed that Zn^{2+} ions incorporated into CdTe lattice to stabilize the surfaces of QDs and reduce the absorption coefficient at the short-wavelength region, i.e. around 400 nm. CdTe and Zn-CdTe QDs exhibited opposite PL respond to Pb^{2+} ions with a concentration about the permissible limit in drinking water. Pb^{2+} could act not only as Z-type ligand coordinating to surficial Te^{2-} or S^{2-} ions but also as GSH scavenger leaving unpassivated Cd^{2+} or Zn^{2+}. Those two effects caused PL decrease in CdTe QDs but PL increase in Zn-CdTe QDs. The PL changes observed in both types of QDs could be utilized to detection of Pb^{2+} ions in water.

Acknowledgements

References

[1] S. A. Elfeky, Facile Sensor for Heavy Metals Based on Thiol-Capped CdTe Quantum Dot, J. Environ, Anal, Chem, Vol. 5, 2018, pp. 1-5, https://doi.org/10.4172/2380-2391.1000232.

[2] P. Yang, F. Dong, Y. Yu, J. Shi, M. Sun, Copper Ion Detection Method Based on a Quantum Dot Fluorescent Probe, Mater. Sci. XX, 2021, pp. 1-6, https://doi.org/10.5755/j02.ms.28024.

[3] H. Li, W. Lu, G. Zhao, B. Song, J. Zhou, W. Dong, G. Han, Silver Ion-doped CdTe Quantum Dots as Fluorescent Probe for Hg2+detection, RSC Adv. 10, 2020, pp. 38965-38973, https://doi.org/10.1039/d0ra07140d.

[4] X. Zhu, Z. Zhao, X. Chi, J. Gao, Facile, Sensitive, and Ratiometric Detection of Mercuric Ions using GSH-capped Semiconductor Quantum Dots, Analyst, Vol. 138, 2013, pp. 3230-3237, https://doi.org/10.1039/c3an00011g.

[5] Y. Zhu, Z. Li, M. Chen, H. M. Cooper, G. Q. Max Lu, Z. P. Xu, One-pot Preparation of Highly Fluorescent Cadmium Telluride/cadmium Sulfide Quantum Dots under Neutral-pH Condition for Biological Applications, J. Colloid Interface Sci. Vol. 390, 2013, pp. 3-10, https://doi.org/10.1016/j.jcis.2012.08.003.

[6] J. Du, X. Li, S. Wang, Y. Wu, X. Hao, C. Xu, X. Zhao, Microwave-assisted Synthesis of Highly Luminescent Glutathione-capped Zn 1-xCd xTe Alloyed Quantum Dots with Excellent Biocompatibility, J. Mater, Chem, Vol. 22, 2012, pp. 11390-11395, https://doi.org/10.1039/c2jm30882g.

[7] S. Najafi, M. Safari, S. Amani, K. Mansouri, M. Shahlaei, Preparation, Characterization and Cell Cytotoxicity of Pd-doped CdTe Quantum Dots and its Application as a Sensitive Fluorescent Nanoprobe, J. Mater, Sci, Mater, Electron, Vol. 30, 2019, pp. 14233-14242, https://doi.org/10.1007/s10854-019-01792-1.

[8] A. Tall, K. R. D. Costa, M. J. de Oliveira, I. Tapsoba, U. Rocha, T. O. Sales, M. O. F. Goulart, J. C. C. Santos, Photoluminescent Nanoprobes Based on Thiols Capped CdTe Quantum Dots for Direct Determination of Thimerosal in Vaccines, Talanta, Vol. 221, 2021, pp. 121545, https://doi.org/10.1016/j.talanta.2020.121545.

[9] D. Das, R. K. Dutta, Photoluminescence Lifetime Based Nickel Ion Detection by Glutathione Capped CdTe/CdS Core-shell Quantum Dots, J. Photochem, Photobiol, A Chem, Vol. 416, 2021, pp. 113323, https://doi.org/10.1016/j.jphotochem.2021.113323.

[10] M. Labeb, A. H. Sakr, M. Soliman, T. M. Abdel-Fattah, S. Ebrahim, Effect of Capping Agent on Selectivity and Sensitivity of CdTe Quantum Dots Optical Sensor for Detection of Mercury Ions, Opt, Mater, Amst, Vol. 79, 2018, pp. 331-335, https://doi.org/10.1016/j.optmat.2018.03.060.

[11] H. Bao, Y. Gong, Z. Li, M. Gao, Enhancement Effect of Illumination on the Photoluminescence of Water-soluble CdTe Nanocrystals: Toward Highly Fluorescent CdTe/CdS Core-shell

Structure, Chem, Mater, Vol. 16, 2004, pp. 3853-3859,

https://doi.org/10.1021/cm049172b.

[12] Y. He, L. M. Sai, H. T. Lu, M. Hu, W. Y. Lai, Q. L. Fan, L. H. Wang, W. Huang, Microwave-assisted Synthesis of Water-dispersed CdTe Nanocrystals with High Luminescent Efficiency and Narrow Size Distribution, Chem, Mater, Vol. 19, 2007, pp. 359-365,

https://doi.org/10.1021/cm061863f.

[13] F. Farahmandzadeh, M. Molaei, M. Karimipour, A. R. Shamsi, Highly Luminescence CdTe/ZnSe Core-shell QDs; Synthesis by a Simple Low Temperature Approach, J. Mater, Sci, Mater, Electron, Vol. 31, 2020, pp. 12382-12388, https://doi.org/10.1007/s10854-020-03784-y.

[14] H. Zare, M. Marandi, S. Fardindoost, V. K. Sharma, A. Yeltik, O. Akhavan, H. V. Demir, N. Taghavinia, High-efficiency CdTe/CdS Core/shell Nanocrystals in Water Enabled by Photo-induced Colloidal Hetero-epitaxy of CdS Shelling at Room Temperature, Nano Res, Vol. 8, 2015, pp. 2317-2328,

https://doi.org/10.1007/s12274-015-0742-x.

[15] A. Samanta, Z. Deng, Y. Liu, Aqueous Synthesis of Glutathione-capped CdTe/CdS/ZnS and CdTe/CdSe/ZnS Core/shell/shell Nanocrystal Heterostructures, Langmuir, Vol. 28, 2012, pp. 8205-8215, https://doi.org/10.1021/la300515a.

[16] M. Ulusoy, J. G. Walter, A. Lavrentieva, I. Kretschmer, L. Sandiford, A. Le Marois, R. Bongartz, P. Aliuos, K. Suhling, F. Stahl, M. Green, T. Scheper, One-pot Aqueous Synthesis of Highly Strained CdTe/CdS/ZnS Nanocrystals and Their Interactions with Cells, RSC Adv, Vol. 5, 2015, pp. 7485-7494,

ttps://doi.org/10.1039/c4ra13386b.

[17] J. Jasieniak, M. Califano, S. E. Watkins, Size-dependent Valence and Conduction Band-edge Energies of Semiconductor Nanocrystals, ACS Nano, Vol. 5, 2011, pp. 5888-5902,

https://doi.org/10.1021/nn201681s.

[18] J. Chang, H. Xia, S. Wu, S. Zhang, Prolonging the Lifetime of Excited Electrons of QDs by Capping them with π-conjugated Thiol Ligands, J. Mater, Chem. C, Vol. 2, 2014, pp. 2939-2943,

https://doi.org/10.1039/c3tc32523g.

[19] J. S. Kamal, A. Omari, K. Van Hoecke, Q. Zhao, A. Vantomme, F. Vanhaecke, R. K. Capek, Z. Hens, Size-Dependent Optical Properties of Zinc Blende Cadmium Telluride.pdf, 2012.

[20] M. Boucharef, S. Benalia, D. Rached, M. Merabet, L. Djoudi, B. Abidri, N. Benkhettou, First-principles Study of the Electronic and Structural Properties of (CdTe)n/(ZnTe)n Superlattices, Superlattices Microstruct, Vol. 75, 2014, pp. 818-830,

https://doi.org/10.1016/j.spmi.2014.09.014.

[21] Y. R. Luo, Comprehensive Handbook of Chemical Bond Energies, Compr, Handb, Chem, Bond Energies, 2007, pp. 1029-1035,

https://doi.org/10.1201/9781420007282.

[22] W. Li, J. Liu, K. Sun, H. Dou, K. Tao, Highly Fluorescent Water Soluble CdxZn1-xTe Alloyed Quantum Dots Prepared in Aqueous Solution: One-step Synthesis and the Alloy Effect of Zn, J. Mater, Chem, Vol. 20, 2010, pp. 2133-2138,

https://doi.org/10.1039/b921686c.

[23] O. Adegoke, E. Y. Park, Size-confined Fixed-composition and Composition-dependent Engineered Band Gap Alloying Induces Different Internal Structures in L-cysteine-capped Alloyed Quaternary CdZnTeS Quantum Dots, Sci, Rep, Vol. 6, 2016, pp.1-9,

https://doi.org/10.1038/srep27288.

[24] J. L. Gautier, J. P. Monrás, I. O. Osorio-Román, C.C. Vásquez, D. Bravo, T. Herranz, J. F. Marco, J. M. Pérez-Donoso, Surface Characterization of GSH-CdTe Quantum Dots, Mater, Chem, Phys, Vol. 140, 2013, pp. 113-118,

https://doi.org/10.1016/j.matchemphys.2013.03.008.

[25] B. R. C. Vale, R. S. Mourão, J. Bettini, J. C. L. Sousa, J. L. Ferrari, P. Reiss, D. Aldakov, M. A. Schiavon, Ligand Induced Switching of the Band Alignment in Aqueous Synthesized CdTe/CdS Core/shell nanocrystals, Sci. Rep. 9, 2019, pp. 1-12,

https://doi.org/10.1038/s41598-019-44787-y.

[26] S. Taniguchi, M. Green, The Room-temperature Structural and Optical Transformation of Cadmium Chalcogenide Quantum Dots Triggered by Reactive Cations, J. Mater, Chem, Vol. 21, 2011, pp. 11592-11598,

https://doi.org/10.1039/c1jm10248f.

[27] N. Kirkwood, J. O. V. Monchen, R. W. Crisp, G. Grimaldi, H. A. C. Bergstein, I. Du Fossé, W. Van Der Stam, I. Infante, A. J. Houtepen, Finding and Fixing Traps in II-VI and III-V Colloidal Quantum Dots: The Importance of Z-Type Ligand Passivation, J. Am, Chem. Soc, Vol. 140, 2018, pp. 15712-15723,

https://doi.org/10.1021/jacs.8b07783.